

## MEASUREMENT OF INTEGRAL CROSS SECTIONS OF SELECTED DOSIMETRY REACTIONS IN LR-0 REACTOR

**Michal Kostal<sup>1</sup>, Tomas Czakoj<sup>1</sup>, Evzen Losa<sup>1</sup>, Martin Schulc<sup>1</sup>, Vlastimil Juříček<sup>1</sup>, Jan Šimon<sup>1</sup>, Vojtěch Rypar<sup>1</sup>, Martin Mareček<sup>1</sup>, Roberto Capote<sup>2</sup>, Andrej Trkov<sup>2</sup>**

<sup>1</sup>Research Center Rez  
Husinec-Řež 130, 250 68, Czech Republic

<sup>2</sup>Nuclear Data Section, International Atomic Energy Agency  
A-1400 Wien, Austria

[michal.kostal@cvrez.cz](mailto:michal.kostal@cvrez.cz), [r.capotenoy@iaea.org](mailto:r.capotenoy@iaea.org)

### ABSTRACT

The cross section is a fundamental quantity which affects the accuracy of Monte Carlo simulations widely used in nuclear applications. A new dosimetry library IRDFF-II that contains cross section evaluations that include full uncertainty quantification is being developed by the International Atomic Energy Agency and expected to be released in January 2020; a preliminary version IRDFF-1.05 was released in 2014 and is being tested in this work. Validation of the cross-section evaluations proposed for this library is a high priority task. The validation can be realized using integral cross sections measured in standard and/or reference neutron benchmark fields. Integral quantities feature significantly lower uncertainties than differential nuclear data. If the neutron spectrum where the cross section is measured is well characterized, then the Spectrum Averaged Cross Section can be used for validating of existing evaluations.

KEYWORDS: LR-0, Spectral Averaged Cross Section, Integral experiment

### 1. INTRODUCTION

There is an extensive set of integral cross sections of dosimetry reactions measured in high power reactors. The advantage of this approach is that even small foils which do not affect the neutron field are significantly activated so that the gamma spectrum can be measured for the irradiated foils in distant geometry. Small foils in distant geometry can be approximated by the point source, thus its activity can be simply measured using experimental detector calibration. However, there may occur significant uncertainties of the power reactor neutron spectrum that make it difficult to use those measurements for data validation. We have developed an innovative approach using the LR-0 reactor, which is a zero-power reactor with low neutron flux. Zero power means that the fuel burn-up is negligible, so there is practically no plutonium accumulated. However, to ensure reliable measurement, enough target nuclei in combination with close measuring geometry must be used. This puts strong requests on the evaluation of measured data. There is need of the precise mathematical core model for flux shift determination between flux monitors' volume and target volume and flux loss and spectral shift in target. Close geometry is also challenging because the precise mathematical model of the detector must be used. If the precise detector geometry is unknown, relevant etalon source should be used, but obtaining such source is practically impossible. The precise model can be employed for determination of both efficiency and coincidence summing correction factor. On the other hand, zero-power reactor has negligible burn-up, thus the neutron field in a well-defined zero power reactor

is a candidate for being defined as a benchmark neutron field. The reference field in the LR-0 reactor is set in the center of a special core, namely in dry irradiation channel surrounded by six 3.3% enriched fuel assemblies. The neutron field can be defined as a reference one, because of well-defined neutron spectrum and neutron flux and also well characterized criticality and core power distribution. Measured dosimetry cross sections are important especially in reactor dosimetry for estimation of the fluxes in reactor pressure vessel.

Measured Spectrum Averaged Cross Section (SACS) can be used either to validate the evaluated reaction cross section (assuming the neutron spectrum is well known), or to validate the neutron spectrum (assuming that the reaction cross sections are well known).

## 2. INSTRUMENTS AND METHODS

The reaction rates used for the derivation of spectrum averaged cross sections (SACS) were determined from the activity of the appropriate nuclide [**Chyba! Nenalezen zdroj odkazů.**]. The normalization to neutron flux was realized using monitor activation foils with well-known cross sections, namely  $^{197}\text{Au}(\text{n},\text{g})$  and  $^{58}\text{Ni}(\text{n},\text{p})$ . Activities were determined using gamma spectrometry. Focus of these measurements was cross sections with E50% (energy limit below which 50% of activation product origins) usually lower than 10 MeV.

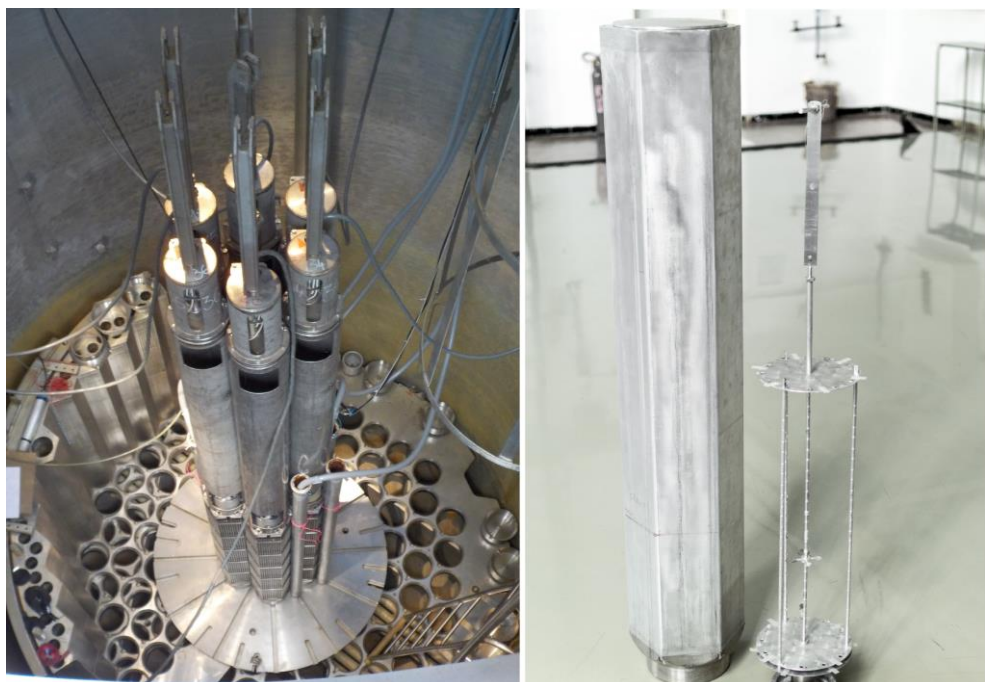


**Figure 1.** Overhead view inside the LR-0 reactor with special core without moderator (left) and view on dry assembly and used holder of activation detectors [2]

### 2.1. Reactor arrangement

The experiments were performed in a specifically designed core assembled in the LR-0 reactor. The LR-0 is a pool-type zero-power light water reactor operated by the Research Centre Řež (Czech Republic). An overhead look of the LR-0 reactor together with axial plot of the core configuration with the dry experimental channel in its center is shown in Figure 1. The core was assembled from six shortened hexagonal (VVER-1000 type) fuel assemblies of the same nominal enrichment (3.3 wt.%  $^{235}\text{U}$ ), where in the center is a dry experimental module with an activation foils holder. Around the core there are placed

dry aluminum tubes for detectors of reactor instrumentations. The control and safety clusters were kept during irradiation totally removed from the core in the upper position, which is 75 cm above the critical moderator level. The cluster guide tube is filled with moderator during operation. Criticality is achieved only by increasing level of moderator. Power control during irradiation is carried out by small changes of moderator level around critical level (less than 0.2 mm). During irradiation the deviations between mean and instantaneous power are most of the time at the interval below  $\pm 1.0\%$ . The operator must change the level approximately every 2 – 3 minutes to compensate the change of reactivity.

The fuel assemblies and experimental module, constructed as a dry hexagonal aluminum tube, have the same outer dimension and are located on a special support plate ensuring lattice pitch 23.6 cm. This ensures the same moderator gap between fuel assemblies and module. The dimensions of the activation foils and the Au power monitor ( $D=3.6\text{mm}$ ,  $\text{th.}=0.1\text{mm}$ ) show that their effect on the perturbation of the neutron flux distribution is negligible.

The irradiation was carried out during approximately 30 hours in three cycles of average reactor power  $\sim 10\text{ W}$  while the neutron flux above 1 MeV in target was  $\sim 4\text{E}7 \text{ cm}^{-2}\cdot\text{s}^{-1}$ . The reaction rates of radioisotopes originating during an irradiation period which is divided into many irradiation cycles can be described by the following equations (1). Whole target arrangement together with flux monitoring foils was placed in the center of this experimental dry channel in the position where the reference neutron field was identified [3]. The field is understand as reference one, because of well-defined criticality [4], neutron flux spatial distribution [4], neutron spectra in core center [5] (Figure 2) and also power distribution in core [6].

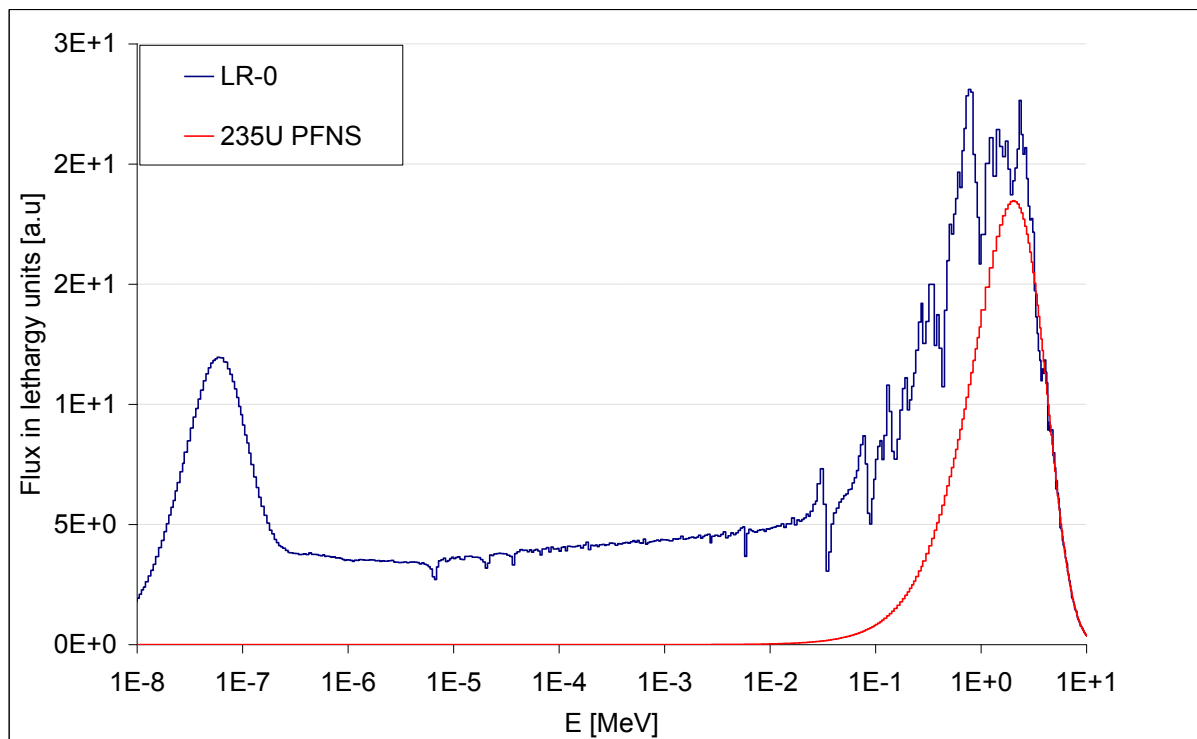


Figure 2. Calculated reactor spectrum and scaled  $^{235}\text{U}$  fission spectrum

## 2.2. Detector Arrangement

The activity of studied activation products as well as flux monitors activities was determined using a gamma spectrometer. HPGe detector (ORTEC) in a vertical configuration with verified material and geometry data was used for all measurements [7]. Due to low induced activities, the most common measuring geometry

was the end cap geometry. Low activities are measurable due to the low background level of the HPGe detector placed in a low-background chamber (a lead shielding with a thin inner copper lining and covered with rubber).

The efficiency calibration was determined by Monte Carlo simulations adjusted to reproduce measured efficiency by fitting the Ge dead layer [8]. The detector model was developed using experimentally obtained parameters from a radiography [9]; the model was validated both for the point etalon and for Marinelli beaker sources. The largest discrepancy between calculated and measured efficiency in relevant gamma energy region is about 1.9 %. Employed detector model also allows a precise derivation of the coincidence summing corrections [10].

### 2.2.1. Gamma spectrometry of irradiated samples

Often, there are many competing reaction channels in irradiated targets which complicate the measurements. This is an issue, e.g., for the  $^{197}\text{Au}(n,2n)$  reaction. The cross section of the  $^{197}\text{Au}(n,g)$  reaction in this arrangement is about 50,000 times larger than the one for the  $^{197}\text{Au}(n,2n)$  reaction. Such ratio does not allow measurement shortly after end of irradiation. As the half-live of  $^{198}\text{Au}$  is shorter than of  $^{196}\text{Au}$ , one of the ways of its measurement is to wait until  $^{198}\text{Au}$  decays. The selecting of proper interval is essential because half-live of  $^{196}\text{Au}$  is not too long.

The time scheme in  $^{60}\text{Co}$  measurement from  $^{63}\text{Cu}(n,\alpha)$  is simpler due to the large  $^{60}\text{Co}$  half-life compared to the 12h half-life of  $^{64}\text{Cu}$ . In the reported experiment, the following targets were used:  $^{\text{nat}}\text{Cu}$ ,  $^{\text{nat}}\text{Fe}$ ,  $^{197}\text{Au}$ ,  $^{\text{nat}}\text{Ti}$ , and  $^{\text{nat}}\text{Ni}$ . Thanks to well-defined setup and well-known spectra the contamination of the used Cu target was determined (Figure 3). It was found that about 46ppm of zinc and 0.2ppm of Ag are present as contaminants. To be sure, the most damaging potential contamination by Co was determined experimentally to be below 0.1ppm by irradiation of the same target material in the silicon filtered thermal neutron beam in the LVR-15 reactor [11]. This result was also confirmed by XRF analysis.

$$q(\bar{P}) = \left( \frac{A(\bar{P})}{A_{\text{Sat}}(\bar{P})} \right)^{-1} \times C(T_m) \times \frac{\lambda}{\varepsilon \times \eta \times N} \times \frac{1}{(1 - e^{-\lambda \cdot T_m})} \times \frac{1}{e^{-\lambda \cdot \Delta T}} \quad (1)$$

$\frac{A(\bar{P})}{A_{\text{Sat}}(\bar{P})} = \sum_i \frac{P^i}{\bar{P}} \times (1 - e^{-\lambda \cdot T_{\text{irr}}^i}) \times e^{-\lambda \cdot T_{\text{end}}^i}$  is relative portion of saturated activity induced during irradiation experiment at fluctuation power P(t)

$q(\bar{P})$  is reaction rate of the activation during power density,  $\bar{P}$  is mean power

$T_m$  is time of measurement by HPGe

$\Delta T$  is time between the end of irradiation and the start of HPGe measurement

$C(T_m)$  is the measured number of counts (NPA)

CSCF is coincidence summing correction factor

$\mathcal{E}$  is the gamma branching ratio

$\eta$  is the detector efficiency (determined with validated model in MCNP6 calculation)

$N$  is the number of target isotope nuclei

$\lambda$  is the decay constant of the radioisotope considered

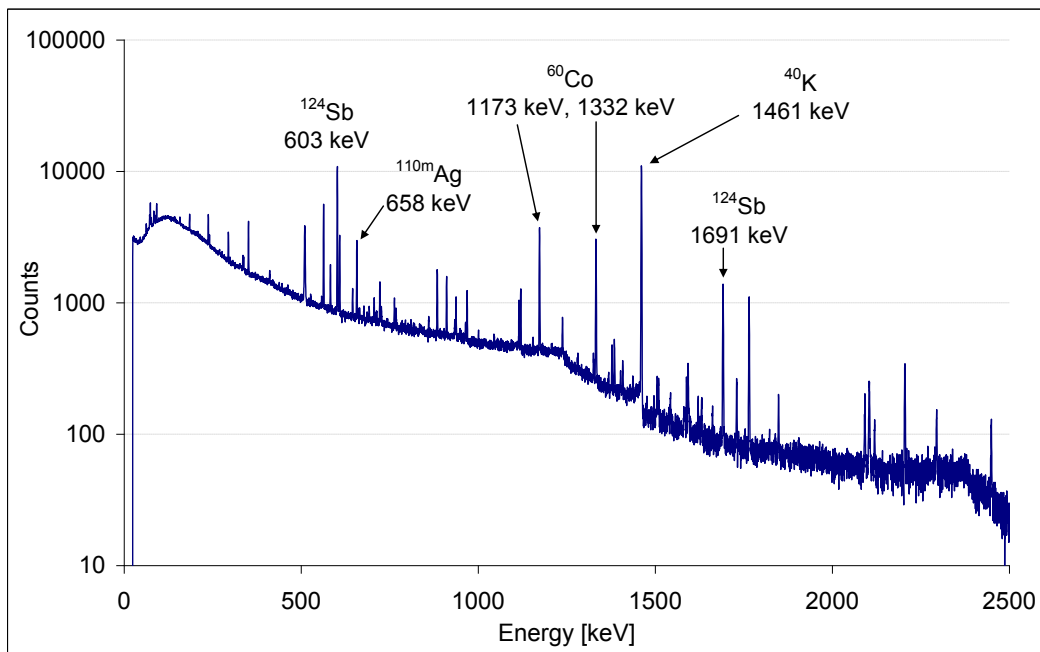


**Figure 3. Gamma spectra of irradiated Cu target**

### 2.2.2. Flux monitors

For the determination of cross sections the reaction rates have to be scaled to unit neutron flux. The actual neutron flux is determined using monitor foils in well-defined geometry. The scaling factor is determined as a ratio between the calculated and measured reaction rates for the monitor foils. This model, which uses numerical scaling factors, allows evaluation of experiments with a larger target arrangement, where the neutron flux in monitoring foils may differ from the flux in the target.

Tantalum and nickel foils with  $^{181}\text{Ta}(\text{n},\text{g})$  and  $^{58}\text{Ni}(\text{n},\text{p})$  reactions were used as monitor. The scaling factors determined from both foils differ only by 0.8%. The basic parameters used for the evaluation of the reaction rates are listed in Table I. Efficiency and CSFC (the Coincidence Summing Factor Correction) were determined using MCNP6, A/Asat is relative portion of saturated activity during irradiation (see Eq. 1), and MCNP determined resonance shielding correction is in the last column.

**Table I. Parameters of targeting and monitoring reactions.**

	Peak [keV]	Efficiency	CSFC	Concentration	A/Asat	Resonance shielding
$^{63}\text{Cu}(\text{n},\alpha)$	1173.0	2.820E-2	0.835	100.0%	0.000412	-
	1332.5	2.550E-2	0.829	100.0%	0.000412	-
$^{197}\text{Au}(\text{n},2\text{n})$	355.0	9.040E-2	0.950	100.0%	0.112134	-
$^{54}\text{Fe}(\text{n},\text{p})$	834.8	4.161E-2	1.000	98.2%	0.002532	-
$^{58}\text{Fe}(\text{n},\text{g})$	1099.2	3.358E-2	0.988	98.2%	0.017475	1.031
$^{47}\text{Ti}(\text{n},\text{p})$	159.4	1.714E-1	1.000	100.0%	0.185254	-
$^{46}\text{Ti}(\text{n},\text{p})$	889.3	4.415E-2	0.819	100.0%	0.009364	-
$^{48}\text{Ti}(\text{n},\text{p})$	983.5	4.069E-2	0.646	100.0%	0.283696	-
	1037.5	3.898E-2	0.638	100.0%	0.283696	-
$^{58}\text{Ni}(\text{n},\text{x})^{57}\text{Co}$	122.0	1.525E-1	1.000	100.0%	0.002908	-
$^{181}\text{Ta}(\text{n},\text{g})$	1121.0	3.562E-2	0.867	100.0%	0.006857	2.289

$^{58}\text{Ni}(\text{n},\text{p})$	1221.4 810.8	3.314E-2 4.627E-2	0.940 0.936	100.0% 100.0%	0.006857 0.011052	2.289 -
-------------------------------------	-----------------	----------------------	----------------	------------------	----------------------	------------

### 2.3. Calculations

The fast neutron fluxes in target arrangements as well as in the monitoring foils were calculated using MCNP6 code [12] in critical mode with ENDF/B VIII.0 nuclear data library [13]. The reaction rates were determined using IRDFF-1.05 cross sections [14, 15]. The  $^{58}\text{Ni}(\text{n},\text{X})^{57}\text{Co}$  reaction is not in IRDFF-1.05, thus data from ENDF/B VIII.0 were used [13]. In the critical mode, the calculations used 1E6 active cycles, 40000 particles were emitted per cycle, and the first 50 cycles were skipped. The single particle (neutron) transport model was used for the simulation of neutron transport in irradiated material. The effect of gamma transport is neglected in this approach, since it has been shown [16] that it is negligible in terms of the  $(\gamma,\text{n})$  reaction contributions to the measured reaction rates. Efficiency curve for used targets and monitors was determined using MCNP6 as well [7]. The calculated statistical uncertainties of all presented results are in all cases below 1 %, thus the MCNP convergence requirements are met.

## 3. RESULTS

The reaction rates, derived from activities using Eq. 1, were normalized per 1 neutron emitted from the core. The experimental results compared with calculations are listed in Table II. Considering that the uncertainties are larger than the C/E-1 values in all cases, the agreement can be taken as excellent. The share of neutrons with energy above 6 MeV in the LR-0 core is 0.708%, while in the  $^{235}\text{U}$  thermal-neutron induced prompt fission neutron spectrum (PFNS) is 2.566%. The limit of 6 MeV reflects the fact that above this energy real LR-0 spectra are indistinguishable from the  $^{235}\text{U}$  PFNS spectra [5] (Figure 4). The ratio between these two numbers is 3.626. It means that when LR-0 spectrum averaged cross sections are scaled by this factor we can obtain the SACS in the reference  $^{235}\text{U}(\text{n}_{\text{th}},\text{f})$  fission spectrum. Derived SACS in the reference  $^{235}\text{U}(\text{n}_{\text{th}},\text{f})$  fission spectrum are listed in Table III. In the same table, measured cross sections are compared with those calculated using IRDFF-1.05 cross sections. For the  $^{58}\text{Ni}(\text{n},\text{X})^{57}\text{Co}$  spectrum averaged cross section, the average value calculated from [17] was used.

**Table II. Evaluated reaction rates in LR-0 spectrum normalized to unit core emissivity and experimental LR-0 spectrum averaged cross section**

	Reaction rate				SACS in LR-0 Experiment
	Experiment	Calculation	C/E-1	Unc.	
$^{63}\text{Cu}(\text{n},\alpha)$	3.09E-32	3.06E-32	-1.0%	3.7%	0.1419
$^{197}\text{Au}(\text{n},2\text{n})$	1.98E-31	1.97E-31	-0.6%	4.4%	0.9097
$^{54}\text{Fe}(\text{n},\text{p})$	4.64E-30	4.63E-30	-0.3%	3.9%	21.32
$^{47}\text{Ti}(\text{n},\text{p})$	1.10E-30	1.10E-30	0.1%	4.1%	5.0482
$^{46}\text{Ti}(\text{n},\text{p})$	6.49E-31	6.59E-31	1.6%	3.6%	2.9823
$^{48}\text{Ti}(\text{n},\text{p})$	1.78E-32	1.74E-32	-2.3%	3.5%	0.0819
$^{58}\text{Ni}(\text{n},\text{x})^{57}\text{Co}$	1.42E-32	1.48E-32	4.3%	12.0%	0.0651
$^{58}\text{Fe}(\text{n},\text{g})$	4.71E-29	4.83E-29	2.5%	3.7%	216.5

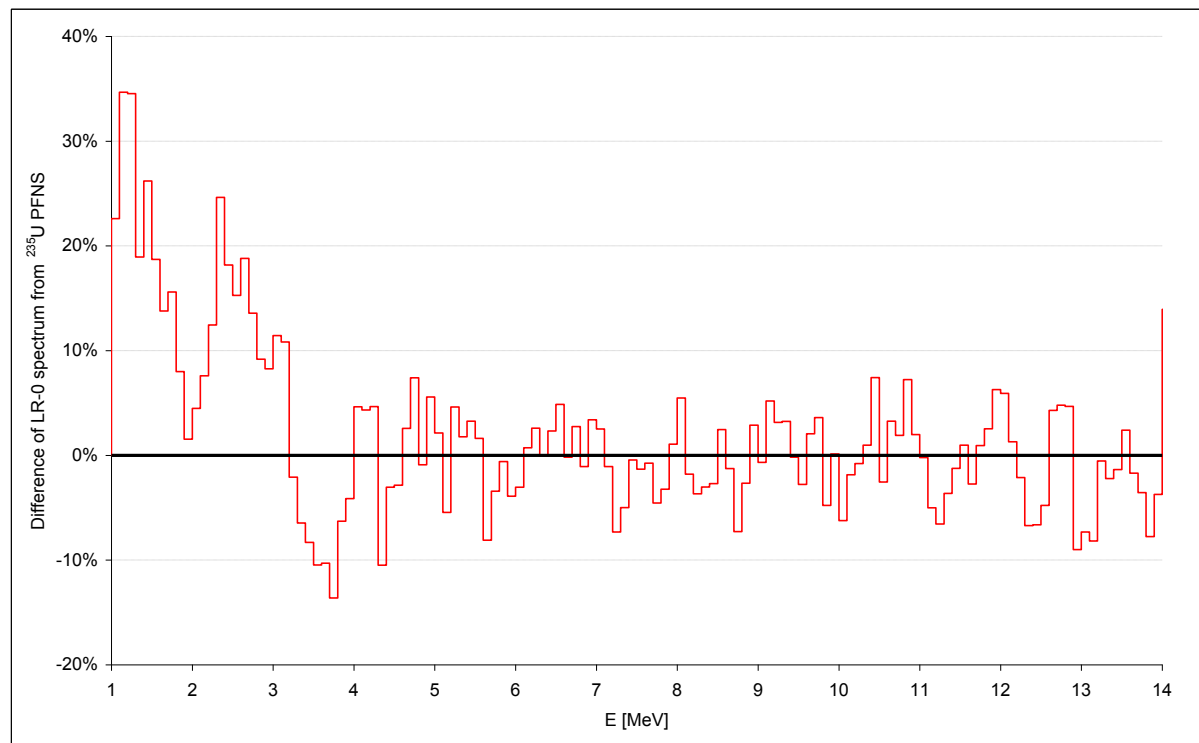


**Figure 4. Difference between calculated reactor spectrum and scaled  $^{235}\text{U}$  fission spectrum**

**Table III. Experimentally determined averaged cross sections scaled to  $^{235}\text{U}$  fission spectrum**

	SACS in $^{235}\text{U}(\text{n}_{\text{th}},\text{f})$ PFNS [mb]	SACS from IRDFF- 1.05 [mb]	C/E-1	Unc.
$^{63}\text{Cu}(\text{n},\text{A})$	0.5144	0.5173	0.6%	3.7%
$^{197}\text{Au}(\text{n},2\text{n})$	3.298	3.387	2.7%	4.4%
$^{54}\text{Fe}(\text{n},\text{p})$	77.31	78.09	1.0%	3.9%
$^{47}\text{Ti}(\text{n},\text{p})$	18.30	17.84	-2.5%	4.1%
$^{46}\text{Ti}(\text{n},\text{p})$	10.81	11.51	6.4%	3.6%
$^{48}\text{Ti}(\text{n},\text{p})$	0.2971	0.3014	1.5%	3.5%
$^{58}\text{Ni}(\text{n},\text{x})^{57}\text{Co}$	0.2360	0.2432	3.1%	12.0%

#### 4. CONCLUSIONS

The measured cross sections are in excellent agreement with calculated ones from the IRDFF-1.05 library. The used simple normalization method allows determining the spectrum averaged cross sections (SACS) even where the neutron spectrum in the target differs from the spectrum seen by the monitor foil. SACS were also determined at lower neutron energies thanks to negligible spectrum oscillations; measured values are in good agreement with SACS in the  $^{235}\text{U}(\text{n}_{\text{th}},\text{f})$  reference neutron field.

## ACKNOWLEDGMENTS

Presented results were obtained with the use of the infrastructure Reactors LVR-15 and LR-0, which is financially supported by the Ministry of Education, Youth and Sports - project LM2015074 and also financially supported by the Ministry of Education, Youth and Sports Czech Republic - project LQ1603 Research for SUSEN. This work has been realized within the SUSEN Project (established in the framework of the European Regional Development Fund (ERDF) in project CZ.1.05/2.1.00/03.0108 and of the European Structural Funds and Investment Funds (ESIF) in the project CZ.02.1.01/0.0/0.0/15\_008/0000293), which is financially supported by the Ministry of Education, Youth and Sports - project LM2015093 Infrastructure SUSEN.

## REFERENCES

1. M. Koštál et al., “VVER-1000 Physics Experiments Hexagonal Lattices (1.275 cm Pitch) of Low Enriched U(3.3 wt.% U235)O2 Fuel Assemblies in Light Water:  $^{75}\text{As}(n, 2n)$ ,  $^{23}\text{Na}(n, 2n)$ ,  $^{90}\text{Zr}(n, 2n)$ ,  $^{89}\text{Y}(n, 2n)$  Reaction Rates”, LR(0)-FUND-RESR-001 CRIT-RRATE (2018), NEA/NSC/DOC(2006)1
2. A. Trkov et al., IRDFF-II: A New Neutron Metrology Library, Nuclear Data Sheets 163, (2020), pp. 1 - 108
3. M. Koštál et al., “Study of graphite reactivity worth on well-defined cores assembled on LR-0 reactor”, *Ann. Nucl. En.*, **87**, (2016), 601–611.
4. M. Koštál et al., “Measurement of various monitors reaction rate in a special core at LR-0 reactor, *Ann. Nucl. En.*, **112**, (2018), 759–768.
5. M. Koštál et al., “On similarity of various reactor spectra and  $^{235}\text{U}$  prompt fission neutron spectrum *Appl. Rad. Isot.*, **135**, (2018), 83–91.
6. M. Koštál et al., “Determining the axial power profile of partly flooded fuel in a compact core assembled in reactor LR-0”, *Ann. Nucl. En.*, **90**, (2016), 450–458.
7. M. Koštál et al., “Validation of zirconium isotopes (n,g) and (n,2n) cross sections in a comprehensive LR-0 reactor operative parameters set”, *Appl. Rad. Isot.*, **128**, (2017), 92–100.
8. Boson et al. “A detailed investigation of HPGe detector response for improved Monte Carlo efficiency calculations”, *NIM-A*, **587**, (2008), 304-314
9. Dryak et al., “Experimental and MC determination of HPGe detector efficiency in the 40–2754 keV energy range for measuring point source geometry with the source-to-detector distance of 25 cm”; *Appl. Rad. Isot.*, **64**, (2006), 1346–1349.
10. Tomarchio et al., “Coincidence-summing correction equations in gamma-ray spectrometry with p-type HPGe detectors”, *Rad. Phys. Chem.*, **80**, (2011), 318–323.
11. J Soltes et al 2016, “The New Facilities for Neutron Radiography at the LVR-15 Reactor“ *J. Phys.: Conf. Ser.*, **746** (2016) 012041
12. T. Goorley et al. “Initial MCNP6 Release Overview”, Nuclear Technology, 180, pp 298-315 (2012).
13. R. Brown D.A. et al., “ENDF/B-VIII.0: The 8<sup>th</sup> Major Release of the Nuclear Reaction Data Library with CIELO-project Cross Sections, New Standards and Thermal Scattering Data”, *Nucl. Data Sheets*, **148**, (2018), 1–142Trkov, “Updating and Extending the IRDF-2002 Dosimetry Library”, *J. ASTM Internat.* **9** (2012) JAI104119.
14. E.M. Zsolnay, R. Capote, H.K. Nolthenius, and A. Trkov, Tech. rep. INDC(NDS)-0616, IAEA, Vienna, 2012.
15. R. Capote, K.I. Zolotarev, V.G. Pronyaev, and A. Trkov, Journal of ASTM International (JAI)- 9, Issue 4, 2012, JAI104119
16. M. Koštál et al., “Measurement and calculation of fast neutron and gamma spectra in well defined cores in LR-0 reactor, *Appl. Rad. Isot.*, **120**, (2017), 45–50.
17. N. L. Maidana, M. S. Dias, L. P. Geraldo, Measurements of U-235 Fission Neutron Spectrum Averaged Cross Sections for Threshold Reactions, *Radiochimica Acta*, 64, 7 - 9 (1994)